DOI: 10.13009/EUCASS2023-879
Aerospace Europe Conference 2023 – 10TH EUCASS – 9TH CEAS

Regolith-based Lunar Habitats - an Engineering Approach to Radiation Shielding

Yulia Akisheva [a†], Yves Gourinat [a], Susanna Guatelli [b],
Cédric Dossat [c], Steven Robin-Chabanne [c], Athina Varotsou [c], Aidan Cowley [d] and Advenit Makaya [e]
[a] Institut Supérieur de l'Aéronautique et de l'Espace
10 Av. Edouard Belin, 31400 Toulouse, France
[b] University of Wollongong, Wollongong, Australia
[c] TRAD Tests & Radiations, Toulouse, France
[d] European Space Agency, EAC
[e] European Space Agency, ESTEC
yulia.akisheva@isae-supaero.fr
[†] Corresponding Author

Abstract
Sustainable human exploration of the Moon will largely rely on in-situ resource utilisation, such as using regolith in habitat construction. This paper investigates the relative effectiveness of polymer-enriched regolith as a radiation shield. Radiation-matter interactions are simulated with RayXpert® software, and the dose equivalent in ICRU-sphere behind a representative wall is calculated. The primary radiation source is Galactic Cosmic Ray protons. Secondary emissions are studied, with main focus on neutrons and protons. This work provides quantitative insight into how much polymer is required to claim a significant improvement in terms of radiation protection when compared to a bare regolith wall.

1. Introduction
All major agencies are invested to support humanity's return to the surface of the Moon. For instance, the European Space Agency (ESA) is developing the Moon Village concept where sustainable exploration is largely based on in-situ resource utilisation (ISRU). The prime candidate for ISRU on the Moon is regolith, or the lunar soil. It is abundant and relatively easily accessible on the surface, thus becoming the perfect source of raw materials. One key utilisation of regolith is habitat construction. Regolith can make up the bulk of a habitat structure, ultimately becoming the main load-carrier material as well as the radiation, thermal and micrometeoritic shield.

This work aims to study the radiation shielding properties of lunar regolith, and assess it from the engineering perspective - considering the feasibility and technological readiness of proposed solutions. Radiation-matter interactions are simulated with RayXpert® software [1]–[3] developed at TRAD Tests & Radiations. The software is a Monte Carlo based user-friendly tool. It allows for selective generation of primary radiation sources, detailed 3D visualisations and energy deposition calculations based on GEANT4 [4] physics. The radiation protection potential is evaluated from the analysis of the total dose equivalent and secondary emissions produced in the habitat wall. In this paper, we investigate the relative effectiveness of polymer-enriched regolith. A significant amount of literature proposes sintering techniques using polymer binders to make regolith bricks that can be arranged to make habitats [5]–[10]. Same literature often highlights the added radiation protection due to polymers' richness in hydrogen. However, to the authors' knowledge, no comprehensive study using Monte Carlo tools and calculating the dose equivalent in the human body has been performed. This paper presents the results of such a study. We calculate the dose equivalent in the ICRU-sphere behind a representative habitat wall. In the first part of the study, the wall is mainly made of regolith and is successively enriched with a polymer binder. In the second part, the polymer is instead added as a layer, behind the bare regolith wall. The primary radiation source is Galactic Cosmic Ray (GCR) protons. Secondary emissions are studied, with main focus on neutron and proton production. This work provides quantitative insight into how much polymer is required to claim a significant improvement in terms of radiation protection when compared to a bare regolith wall. From the engineering point of view, simple yet effective solutions can be achieved with cost-effective and radioprotective characteristics if multilayers are used. While polymer binders are a competitive option in terms of time effectiveness, the energy and infrastructure required remain a major concern for construction on the Moon. The research question of this study is:

DOI: 10.13009/EUCASS2023-879

How much (i.e. %wt) polyethylene (PE) is required to effectively improve radiation protection of a regolith-based habitat wall on the Moon; and what is more effective – adding polymers as adhesives into the regolith mix or as separate layers inside a regolith habitat?

The rest of this Section introduces the lunar radiation environment, radiation dose limits used in human spaceflight and lunar surface habitat structures. Section 2 details the numerical model used in this work: radiation, geometrical setup, material definition, and the dose equivalent calculations. Section 3 presents the results. Limitations are discussed in Section 4, where improvements in future work are outlined. Section 5 concludes the study.

1.1 Radiation environment

The primary radiation on the Moon consists of the ever-present Galactic Cosmic Rays, solar wind, and occasional Solar Particle Events (SPEs). The Sun continuously emits the solar wind which consists mainly of protons and electrons of energies that are stopped in very thin shielding. Due to that, the solar wind is typically not considered in radiation protection studies for deep space [11]. The following sub-sections explain GCRs and SPEs in more detail.

When primary radiation comes across matter, such as a shield or the lunar surface, it creates secondary emissions from electromagnetic and nuclear particle interactions. An example of secondary emissions is the lunar albedo. However, it is commonly regarded as a primary source in literature because of its enduring presence.

To address the research question of this paper, only the GCR component is considered in the numerical model, as detailed in Section 2.1. The main radiation source on a long-term exploration mission at the lunar surface is the GCRs, which is enough for a relative analysis of polymer-enriched regolith's effectiveness as a radiation shield.

1.1.1 Galactic Cosmic Rays

At present time, GCRs are believed to originate from supernova explosions with supernova remnants (SNRs) being the sources of GCRs [12], [13]. The diffusive shock acceleration model or the 1st order Fermi mechanism is used to explain the propagation and acceleration of the rays as they travel through space and encounter the effects of other supernova explosions [13], [14]. Simply put, the rays get accelerated through space by the shock waves of new explosions. GCRs are mainly atomic nuclei, mostly protons and He nuclei, stretching over the periodic table and including traces of heavy elements [14]. About 2% of all GCRs are electrons, and the rest are baryons. Out of baryons, 85% are protons, 14% are He ions and the rest are heavier ions. The energy spectrum spans from below 1 MeV to above 10^{20} eV [13], [14]. As the energy increases, the flux intensity of GCRs drops significantly. For instance at 100 MeV, the probability of encountering a particle is 1/cm²/sec and at 10^{20} eV, it is about 1/km²/century [13], [14] as can be seen in Figure 1 from [14].

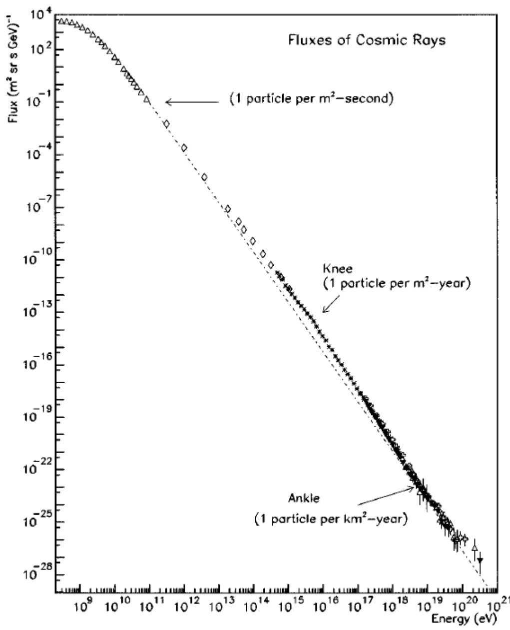

Figure 1: Spectrum of GCRs greater than 100 MeV. The image is taken from [14] - Figure 1

DOI: 10.13009/EUCASS2023-879

1.1.2 Lunar albedo

Resulting from continuous bombardment by GCRs, secondary emissions are ejected in and from the lunar soil in all directions. This component of secondary radiation is called the lunar albedo, and sometimes it is specified as the neutron albedo as it contains a substantial number of neutrons. Some estimations evaluate the dose contribution from the lunar albedo up to 20% [15].

1.1.3 Solar Particle Events

Especially during the periods of high activity, the Sun's ejected protons can be accelerated by the shock of a coronal mass ejection (CME) or during a solar flare to very high energies [16]. SPEs contain protons and also include helium ions as well as high atomic number and energy (HZE) ions. The fluence of protons above 30 MeV can exceed 10^{10} cm^{-2} over several hours or days. Most of these protons have energies of a few tens to hundreds MeV and do not exceed 1 GeV [17].

Although related to the intensity level of solar activity, SPEs are largely unpredictable. This is explained through the complexity of forecasting complex solar and space physics related to particle acceleration during a solar flare or a CME [17]. Taking SPEs into account for future long-term exploration type missions is complex. Typically, an SPE-shelter solution is considered for space vehicle and habitat design, where astronauts would wait the event out. Such shelters are aimed to stop the incoming protons and are likely to have thick walls.

1.2 Radiation dose limits

Radiation protection of astronauts follows the As Low As Reasonably Achievable (ALARA) principle: reduce the exposure as much as feasible for a given mission scenario. Also, the whole-body and some organ doses cannot surpass the dose limits set by space agencies of astronauts. Currently, there are no international limits for deep space missions. Expert and topical teams from different space agencies are looking to develop such limits to support international cooperation in human spaceflight to the Moon and beyond [18].

The dose limits that guide this work are the 30-day whole-body exposure of 250 mSv set by National Aeronautics and Space Administration (NASA) and the 250 mGy-Eq limit on blood-forming organs [19]. The career limit of 1 Sv for ESA astronauts must also be respected [18]. As a guiding principle, although not a dose limit, the authors also cross-check against the exposure on the International Space Station (ISS), which here is considered to be 90-140 mSv per 6 months (based on [20]–[25]).

1.3 Lunar habitats

Lunar habitats may take several forms in the future. Design concepts range from inflatable structures covered with regolith to repurposed lander parts and underground stations. Each design type corresponds to a particular mission, considering its objectives, destination, duration and crew.

In this work, a habitat on the Moon is a hemispheric dome. The full model of a habitat (see Figure 9) consists of a regolith-based dome mounted on top of a large part of lunar soil to generate the lunar albedo during simulations. However, for studying the research question of this paper, a small representation of the habitat wall is enough. A representative brick of lunar regolith simulant is used.

2. Numerical model

2.1 Primary radiation

Primary radiation considered here is the protons of Galactic Cosmic Rays. GCRs mainly consist of protons (shown in Figure 2). The proton energy spectrum stretches up to several TeV [11], however the particle flux drops significantly with increase in energy levels. In this work, the energy spectrum used is presented in Figure 3. It was generated in SPENVIS [26], [27] for free space environment at 1 Astronomical Unit during the 1986-87 solar minimum with the ISO-15390 standard model. To achieve an acceptable level of statistical errors in the results, 1E6 primary particles were used in simulations.

DOI: 10.13009/EUCASS2023-879

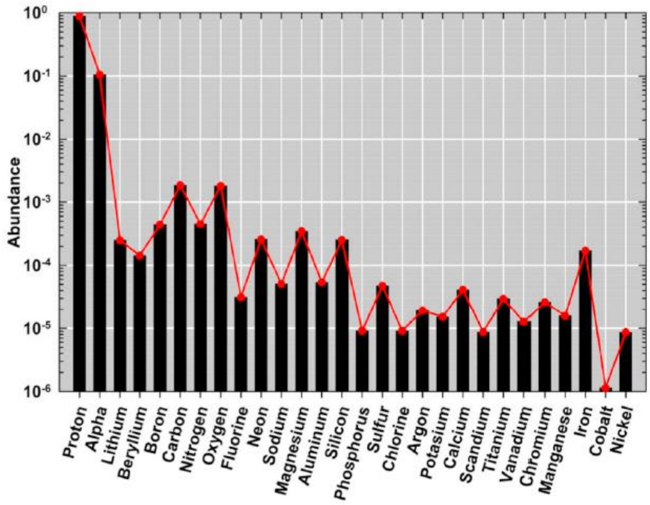

Figure 2: The most abundant GCR ions; image copied from [28]

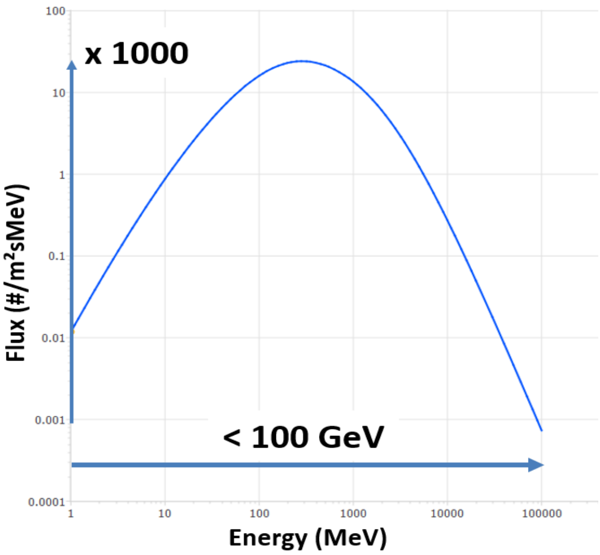

Figure 3: GCR proton energy spectrum used in this work

Considering only the proton component of primary radiation in space is a simplification justified by the higher abundance of hydrogen among all the GCR ions. Furthermore, elements with higher atomic number will be stopped early in thick shields. The habitat wall considered in this work is 50 cm thick for all regolith-based materials.

2.2 RayXpert® tool

RayXpert® is a 3D Monte Carlo tool [1], [3], [29]. The radiation-matter interaction models are based on GEANT4 [4] physics and deal with neutrons, electrons and positrons as well as photons in energy ranges from keV to a hundred MeV.

RayXpert® was originally developed for terrestrial applications in the nuclear and medical fields to provide accurate estimations of dose spatial distributions and dose rates. For this work, TRAD Tests & Radiations is developing a version of RayXpert® specifically designed for space applications [30]. Transport models for alpha particles, protons, heavier ions and neutrons are added, as well as electromagnetic particle interactions, in order to effectively represent space radiation environment and its physics.

DOI: 10.13009/EUCASS2023-879

2.3 Geometrical setup

The focus of this study is to perform relative analysis of radiation protection effectiveness of polymer-enriched regolith. A simplified representation of the habitat wall and incoming radiation is selected. Only a part of the wall is used because the geometry is symmetrical and it allows to reduce the computational power required to run simulations. The setup in RayXpert® is shown in Figure 4. Due to the simplified geometry, it is considered that the radiation field comes in parallel and perpendicular to the surface of the habitat wall. The field is larger than the sensitive volume (ICRU sphere here) to encompass it. The wall is larger than the radiation beam in the field of view of the beam to account for particle scattering. The dimensions of the elements are:

- Sensitive volume: 30 cm diameter sphere
- Habitat wall: 80x80 cm in the field of view of the beam, and 50 cm thick
- Radiation beam: 40x40 cm

The simulations are set in vacuum to represent the lunar environment.

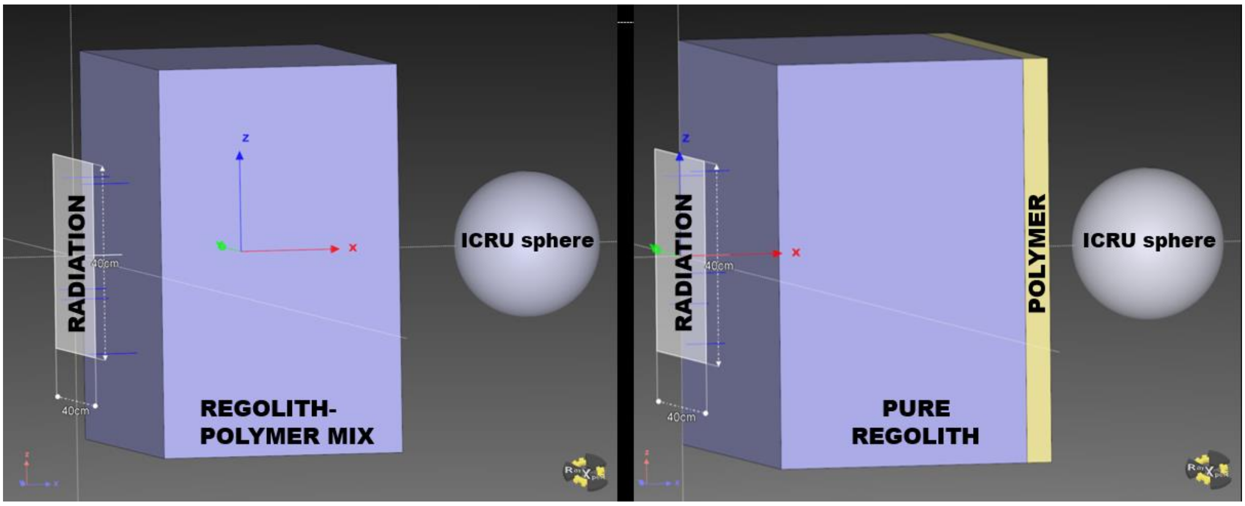

Figure 4: Simulation setup in RayXpert®, left – enrichment, right – multilayers

As outlined in the Introduction, there are two parts in this study: the **regolith enrichment** when polyethylene is added to make a regolith-polymer mix, and **multilayers** when polyethylene is added as a separate layer behind a bare brick of regolith. The results are then cross-compared between the two parts to study the relative effectiveness of polymer-enriched regolith Vs multilayers. Table 1 presents the thicknesses of polyethylene layers (right side in Figure 4), equivalent in mass to the polyethylene added to regolith (left side in Figure 4).

Table 1: Polyethylene layer thicknesses, equivalent in mass to the added polyethylene into regolith

	Equivalent thickness of PE layer (cm)
1% PE	**0.78**
2% PE	**1.56**
5% PE	**3.90**
10% PE	**7.80**
20% PE	**15.59**
30% PE	**23.39**
50% PE	**38.98**

2.4 Material definition

Regolith simulant used in this work is the EAC-1A [31]. Its chemical composition (see Table 2) and nominal bulk density of 1.45 g/cm³ are used as the baseline regolith model. For numerical simulations, the element composition of regolith is used as reported in Table 3.

DOI: 10.13009/EUCASS2023-879

Table 2: EAC-1A simulant's chemical composition, from [31]

	Al_2O_3	CaO	FeO	K_2O	MgO	MnO	Na_2O	P_2O_5	SiO_2	TiO_2	Total
wt%	12.6	10.8	12	1.3	11.9	0.2	2.9	0.6	43.7	2.4	98.4

Table 3: Bare regolith's chemical composition as used in this work

	O	Al	Ca	Fe	K	Mg	Mn	Na	P	Si	Ti	Total
Fraction (%)	42.96	6.67	7.72	9.33	1.08	7.18	0.15	2.15	0.26	20.43	2.07	100.0

The polyethylene formula used here is $(C_2H_4)_n$ and its density is 0.93 g/cm³. As polyethylene is added to regolith, the final mixture's density is always kept at 1.45 g/cm³. Hence, the fraction of constituent elements changes in the model, according to the percentage of polyethylene in the mix. This is done to keep the same aerial density of 72.5 g/cm² in all the cases of regolith enrichment as well as in the bare regolith brick in the case of multilayers. This way, the results can be cross-compared to evaluate the different materials vis-à-vis their radiation protection effectiveness.

The ICRU sphere is defined as a 30 cm diameter sphere made of ICRU tissue. The tissue is 1 g/cm³ dense and consists of 76.2% oxygen, 11.1% carbon, 10.1% hydrogen, and 2.6% nitrogen [11]. The ICRU sphere serves as the first approximation of radiation exposure in the human body.

2.5 Dose equivalent

From the deposited energy and absorbed dose inside the sensitive volume, a dimensionless factor is used to calculate the dose equivalent in the representative tissue. The dose equivalent considers the biological effectiveness of radiation which depends on the radiation type and energy.

Due to the mixed nature of radiation in space, [32] suggests using Q(LET) quality factors as a function of linear energy transfer (LET) to calculate the dose equivalent in organs and tissues. They are based on the ICRP_60 factors, which are given for each particle type in all different organ types (and the two genders) and discretised by particle energy. When using these factors, the dose equivalent, H (in Sv) is calculated as:

$$H = Q(LET)D \tag{1}$$

where D is the absorbed dose at the point of interest in tissues and Q(LET) is defined in ICRP1991 [33] as:

$$Q(LET) = \begin{cases} 1 & LET \quad 10 \, \langle \, keV/\mu m \\ 0.32LET - 2.2 \quad for \quad 10 & \leq LET \quad \leq 100 \quad keV/\mu m \\ 300/\sqrt{LET} & LET \quad 100 \, \rangle \, keV/\mu m \end{cases} \tag{2}$$

3. Results

The results of the first case – regolith enrichment with polyethylene – are summarised in Figure 5 and Table 4. The errors for all points are below 1.2% and error bars are included. The total dose equivalent is the sum of the doses from all primary and secondary particles considered: protons, neutrons, electrons, photons, positrons, alpha, deutons, tritons, He3, and heavier ions. Only the doses due to protons and neutrons are presented because their combined part in the total dose is around 93% in all cases (see Table 4). It is evident that the total dose equivalent does not decrease significantly when PE is added to regolith. More than 30% of PE is required to consistently reduce the dose beyond the statistical error. It can be seen that, although weak, there is a tendency to reduce the proton contribution to the total dose when the concentration of PE is high (above 30%).

DOI: 10.13009/EUCASS2023-879

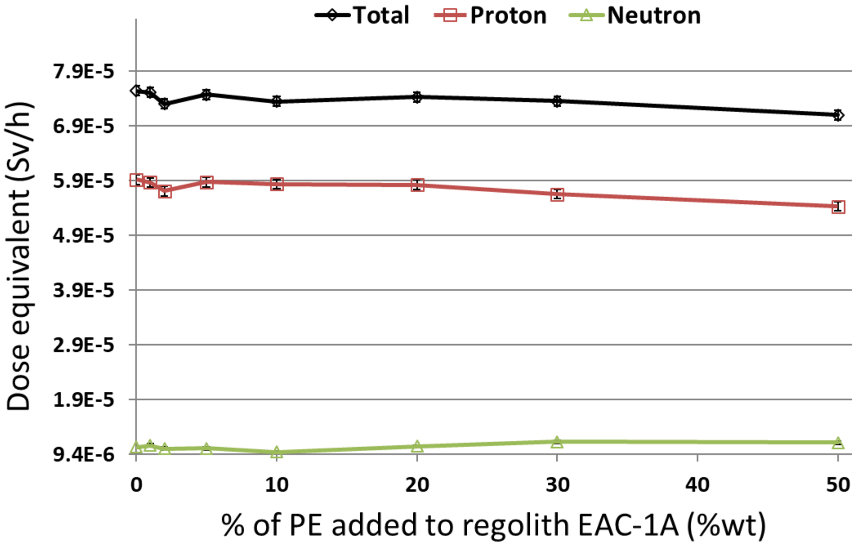

Figure 5: Dose equivalent in ICRU sphere as a function of regolith composition when polyethylene (PE) is added to EAC-1A

Table 4: Results of the total dose equivalent in ICRU sphere for the case of regolith enrichment with PE

Regolith wall	**Total Dose eq. (Sv/h) ICRU sphere**	**Total dose eq./total dose eq. in bare regolith (%)**	**Proton/Total Dose eq. (%)**	**Neutron/Total Dose eq. (%)**
bare regolith (50 cm)	7.58E-05	**-**	79%	14%
1% PE	7.55E-05	**100%**	78%	15%
2% PE	7.34E-05	**97%**	78%	14%
5% PE	7.51E-05	**99%**	79%	14%
10% PE	7.39E-05	**97%**	80%	13%
20% PE	7.47E-05	**99%**	78%	14%
30% PE	7.39E-05	**97%**	77%	16%
50% PE	7.14E-05	**94%**	77%	16%

Figure 6 superposes the results in Figure 5 and the study of multilayers. The error bars are included and all errors are under 1.2%. It is apparent how both the total and proton dose equivalent are reduced with thicker layers of PE. Since the layers are equivalent in mass to the PE added to regolith in the enrichment case, it is evident that adding layers of PE is more efficient for radiation protection from GCR protons than adding equivalent mass of PE into the regolith powder mix.

DOI: 10.13009/EUCASS2023-879

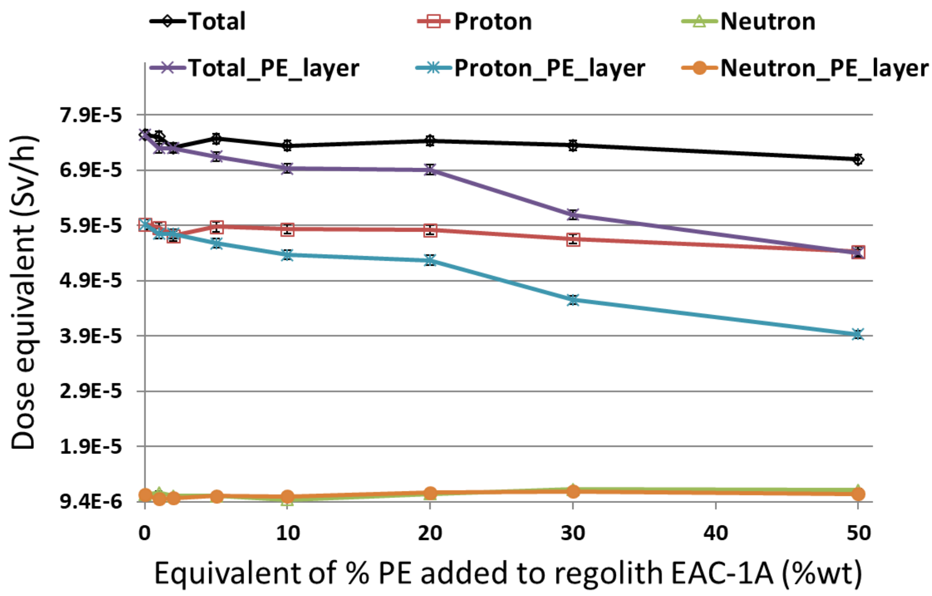

Figure 6: Dose equivalent in ICRU sphere as a function of regolith composition when polyethylene (PE) is added to EAC-1A and for equivalent PE layers behind 50 cm regolith block

Table 5 justifies the effectiveness of multilayers as already in the case of 0.78 cm – the thinnest layer studied, which corresponds to the case of adding 1% PE to enrich regolith, produces a dose reduction larger than the 30% enrichment case. Despite the fact that thick PE layers reduce the total dose significantly, it is not advised to consider layers thicker than 4-5 cm due to technical feasibility and cost. The wall of **50 cm regolith and 4 cm of polyethylene** is considered as a **reference solution** as it reduces the total dose equivalent by about 5%.

Table 5: Results of the total dose equivalent in ICRU sphere for the case of polyethylene layers

Regolith wall	Total Dose eq. (Sv/h) ICRU sphere	Total dose eq./total dose eq. in bare regolith (%)	Proton/Total Dose eq. (%)	Neutron/Total Dose eq. (%)
50 cm regolith	7.58E-05	-	79%	14%
50 cm reg. 0.78 cm PE	7.34E-05	**96.75%**	78.92%	13.52%
50 cm reg. 1.56 cm PE	7.34E-05	**96.77%**	78.85%	13.67%
50 cm reg. 3.9 cm PE	7.19E-05	**94.80%**	78.16%	14.47%
50 cm reg. 7.8 cm PE	6.97E-05	**91.93%**	77.59%	14.86%
50 cm reg. 15.6 cm PE	6.95E-05	**91.59%**	76.48%	15.90%
50 cm reg. 23.4 cm PE	6.14E-05	**80.92%**	74.84%	18.39%
50 cm reg. 39 cm PE	5.44E-05	**71.75%**	72.99%	19.86%

Figure 7 and Figure 8 present the flux of protons and neutrons (respectively) as detected in the ICRU sphere. The protons are both primary and secondary. Hence, it is difficult to make a conclusive statement about the exact effect of PE on GCR protons. However, consequent simulations showed that protons up to 200 MeV are stopped in polyethylene. It is also considered that higher-energy protons are decelerated through the PE layer.

The effect of a PE layer on the epithermal and fast neutrons dose reduction seems to be negligible. Table 5 indicates that the contributions to the total dose from neutrons is slightly larger in the case of a 3.9 cm PE layer, if compared to bare regolith. Figure 8 shows how this contribution to the dose originates from thermal neutrons as their flux is considerably higher in the case of an added PE layer – between one and two orders of magnitude across the part of the energy spectrum.

DOI: 10.13009/EUCASS2023-879

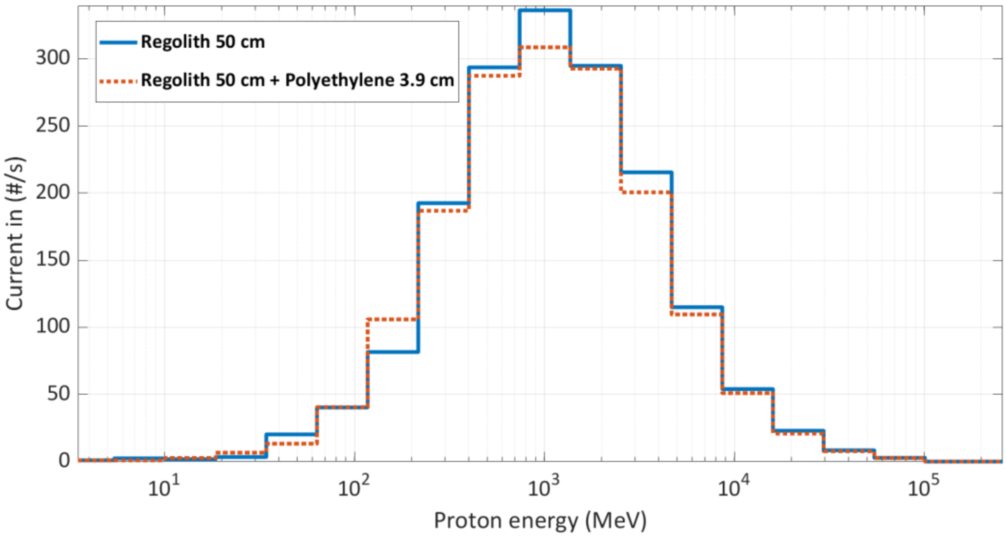

Figure 7: Proton flux in ICRU sphere

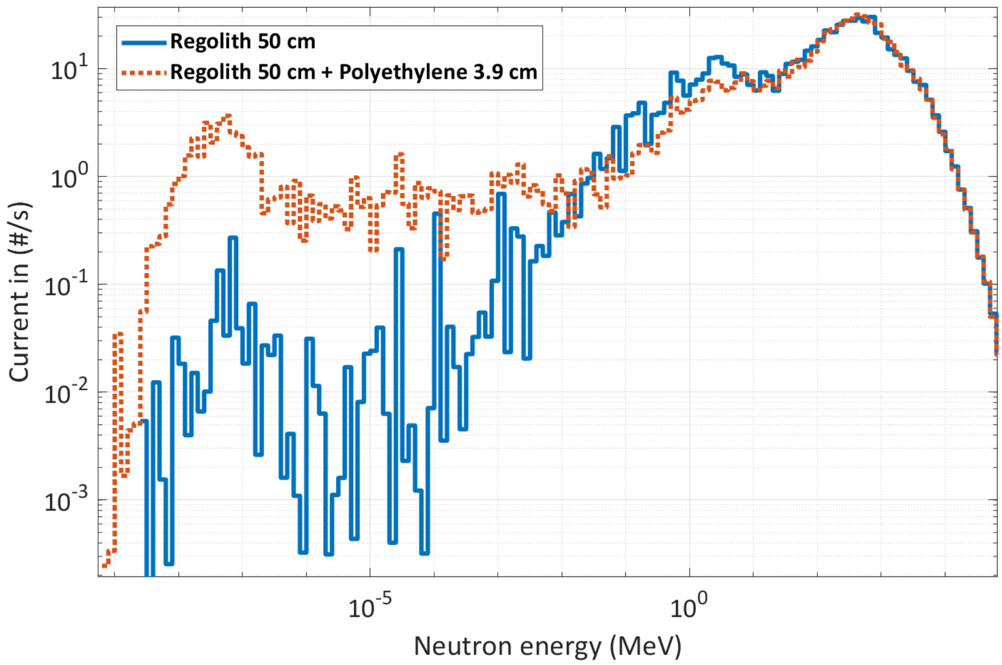

Figure 8: Neutron flux in ICRU sphere

As detailed in Table 6 for all cases of PE layers, the extrapolated dose equivalent after 30 days does not exceed the 250 mSv limit. Even considering the limitations in Section 4, the reference scenario of 50 cm of regolith and 4 cm of PE is well within the limits. However, looking at the cumulated dose in 180 days, it exceeds the reference exposure of 90 – 140 mSv on the ISS. Further investigations into thicker regolith layers as well as alternation of the layers are advised.

DOI: 10.13009/EUCASS2023-879

Table 6: Dose equivalent in ICRU sphere for the case of multilayers

	Dose equivalent in ICRU sphere		
	mSv/d	**mSv/30d**	**mSv/180d**
50 cm regolith	1.82	54.6	327.6
50 cm reg. 0.78 cm PE	1.76	52.8	316.9
50 cm reg. 1.56 cm PE	1.76	52.8	317.0
50 cm reg. 3.9 cm PE	1.73	51.8	310.6
50 cm reg. 7.8 cm PE	1.67	50.2	301.2
50 cm reg. 15.6 cm PE	1.67	50.0	300.1
50 cm reg. 23.4 cm PE	1.47	44.2	265.1
50 cm reg. 39 cm PE	1.31	39.2	235.1

4. Consideration of limitations

The following points consider the main limitations of the work presented in this paper. Each point considers improvements and suggests how to develop future work.

- While GCR protons are the most abundant sources of primary radiation in outer space, other ions should be considered for full analysis. The suggestion for future work is to first estimate the contribution to the dose from the helium, carbon and iron ions. These four elements (including hydrogen), will serve as a first representation the full ion spectrum of GCRs – covering the light and heavy atomic weight ions with their relative abundances in space. As indicated in the Section 2.1, heavy ions are likely to be stopped in the thick shielding of the habitat wall. However, they will generate secondary radiations in the wall. Therefore, full analysis should also include GCR ions other than hydrogen. This is addressed in the on-going work of the authors.
- Solar Particle Events are not considered in this work. Full analysis should consider a design case of SPEs. Unpublished work of the authors will provide insights into the contribution to the dose from the case of October 1989 SPE series. It will be demonstrated that beyond thick shielding, as the case in this work, such events will not represent a significant danger for astronaut radiation exposure during a representative six-months mission on the surface of the Moon.
- The model represents a small part of a hemispheric habitat. It is assumed that due to representative size of the regolith slab, the incoming radiation will be incident in parallel rays, perpendicular to the shielding surface. This is a simplified design. For completeness, the full model of a hemispheric dome on a large patch of lunar soil should be adopted to generate the lunar albedo in numerical simulations (see Figure 9). The incident radiation will then be isotropic as coming from the outer space. Such a model is part of the on-going work of the authors.
- The numerical model is set in vacuum. In reality inside the habitat, there will be breathable air. Some of the secondary emissions will have shorter paths in air than they do in vacuum, e.g. alpha particles. Therefore, the dose calculated inside the ICRU sphere is likely an overestimation in respect to such secondary emissions.
- The primary spectrum is taken from SPENVIS and the full spectrum is used unaccounted for the partial shielding from the Moon. In reality, a large portion (up to 2π) of the spectrum is not going to reach the habitat on the surface because the Moon will shield from radiation coming from the other side. Considering the full 4π spectrum incident on the wall is an over estimation. It can be considered that the results are an over estimation of the dose equivalent from GCR protons. Running a full 3D model with the habitat on top of the lunar surface (example shown in Figure 9) would estimate the extend of the over estimation.
- Full models should contain human phantoms of both biological sexes instead of the ICRU sphere. It will improve the understanding of radiation exposure to organs and tissues, as well as gain insights into possible sex differences. However, in order to estimate the overall exposure limits during a long-duration mission, the ICRU sphere serves as a good proxy.

DOI: 10.13009/EUCASS2023-879

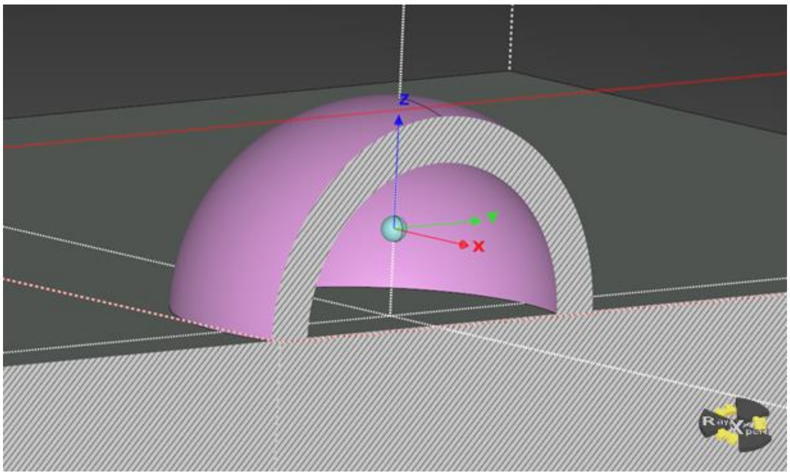

Figure 9: Model of a hemispheric habitat on the lunar surface with the ICRU sphere inside

5. Conclusions

At least 30-50% of PE by mass would be required to consider an *effective* advantage in radiation protection vis-à-vis bare regolith. Adding more than 50% would question the extend of ISRU in habitat construction. Cited literature reports using 1-10% of added adhesives to make bricks of regolith. Given the state-of-art, this paper concludes that adding polymers such as polyethylene does not improve radiation protection properties of the construction. An overarching recommendation for colleagues in the space community is to perform Monte Carlo analysis similar to the one detailed in this paper in order to be able to state conclusively if the proposed ISRU techniques indeed offer an improvement in radiation protection or not.

It is advised to keep the reference of 4 cm of PE in case of multilayers. Thicker layers provide better protection but making such constructions on the Moon will be costly and complex. It is estimated that to cover a small habitat for one astronaut would require about 1.7 ton of polyethylene to be brought, or repurposed, from Earth. This mass corresponds to a hemispheric PE layer measuring 4 cm in thickness and covering 40 m^3. Having 4 cm of polyethylene behind 50 cm of regolith reduces the total dose equivalent in ICRU by 4-5% when compared to the case of bare 50 cm of regolith.

Regarding the research question of this paper, it can be concluded that within the scope of assumptions and limitations, multilayer solutions are far better in terms of radiation protection than the enriched regolith options. Future and on-going work, as outlined in Section 4 will detail the findings, considering the fuller GCR spectrum, the SPE contribution to doses, and alternative configuration of regolith and polyethylene layers.

Acknowledgements

This study is supported by the European Space Agency, TRAD Tests & Radiations, and the Department of Mechanics of Structures and Materials of ISAE-SUPAERO under the ESA OSIP collaboration on the Protective Use of Regolith for Planetary and Lunar Exploration (PURPLE) PhD project. It is also supported by the University of Wollongong. The authors would like to thank all entities for their contribution to this project.

The corresponding author would like to extend special thanks to the ever-growing support of Pablo Ramón Sánchez Chisvert. Furthermore, the author would like to thank an aspiring astrophysicist Mohamed Amine Ezzine for support and proof-reading this article.

References

[1] S. Derreumaux, S. Vecchiola, T. Geoffray, and C. Etard, “Evaluation of RayXpert® for shielding design of medical facilities,” in *13th International Conference on Radiation Shielding (ICRS-13) & 19th Topical Meeting of the Radiation Protection & Shielding Division of the American Nuclear Society -2016 (RPSD-2016)*, Paris, France, Oct. 2016, p. 06024. doi: 10.1051/epjconf/201715306024.

[2] B. Simony, “RayXpert v1.8 User’s guide,” TRAD Tests & Radiations, TRAD/DL/DOS/RAYXPERT/CD/110412 rev17, Nov. 2020.

[3] “RayXpert 3D modeling and dose calculation software using a Monte Carlo,” *RayXpert*. https://www.rayxpert.com/en/ (accessed Sep. 02, 2022).

[4] S. Agostinelli *et al.*, “Geant4—a simulation toolkit,” *Nuclear Instruments and Methods in Physics Research Section A: Accelerators, Spectrometers, Detectors and Associated Equipment*, vol. 506, no. 3, pp. 250–303, Jul. 2003, doi: 10.1016/S0168-9002(03)01368-8.

DOI: 10.13009/EUCASS2023-879

[5] C. Montes *et al.*, “Evaluation of lunar regolith geopolymer binder as a radioactive shielding material for space exploration applications,” *Advances in Space Research*, vol. 56, no. 6, pp. 1212–1221, Sep. 2015, doi: 10.1016/j.asr.2015.05.044.

[6] T. Sik Lee, J. Lee, and K. Yong Ann, “Manufacture of polymeric concrete on the Moon,” *Acta Astronautica*, vol. 114, pp. 60–64, Sep. 2015, doi: 10.1016/j.actaastro.2015.04.004.

[7] M. Isachenkov, S. Chugunov, I. Akhatov, and I. Shishkovsky, “Regolith-based additive manufacturing for sustainable development of lunar infrastructure – An overview,” *Acta Astronautica*, vol. 180, pp. 650–678, Mar. 2021, doi: 10.1016/j.actaastro.2021.01.005.

[8] J. Lee, K. Y. Ann, T. S. Lee, and B. B. Mitikie, “Bottom-up heating method for producing polyethylene lunar concrete in lunar environment,” *Advances in Space Research*, vol. 62, no. 1, pp. 164–173, Jul. 2018, doi: 10.1016/j.asr.2018.03.039.

[9] G. Cesaretti, E. Dini, X. De Kestelier, V. Colla, and L. Pambaguian, “Building components for an outpost on the Lunar soil by means of a novel 3D printing technology,” *Acta Astronautica*, vol. 93, pp. 430–450, Jan. 2014, doi: 10.1016/j.actaastro.2013.07.034.

[10] T. Chen, B. J. Chow, Y. Zhong, M. Wang, R. Kou, and Y. Qiao, “Formation of polymer micro-agglomerations in ultralow-binder-content composite based on lunar soil simulant,” *Advances in Space Research*, vol. 61, no. 3, pp. 830–836, Feb. 2018, doi: 10.1016/j.asr.2017.10.050.

[11] ICRP, “Assessment of radiation exposure of astronauts in space. ICRP Publication 123,” 42(4), 2013.

[12] P. Blasi, “Origin of Galactic Cosmic Rays,” *Nuclear Physics B - Proceedings Supplements*, vol. 239–240, pp. 140–147, Jun. 2013, doi: 10.1016/j.nuclphysbps.2013.05.023.

[13] E. Amato, “The origin of galactic cosmic rays,” *Int. J. Mod. Phys. D*, vol. 23, no. 07, p. 1430013, Jun. 2014, doi: 10.1142/S0218271814300134.

[14] J. W. Cronin, “Cosmic rays: the most energetic particles in the universe,” *Cosmic rays*, vol. 71, no. 2, p. 8, 1999.

[15] T. P. Dachev *et al.*, “An overview of RADOM results for earth and moon radiation environment on Chandrayaan-1 satellite,” *Advances in Space Research*, vol. 48, no. 5, pp. 779–791, Sep. 2011, doi: 10.1016/j.asr.2011.05.009.

[16] A. Anastasiadis, D. Lario, A. Papaioannou, A. Kouloumvakos, and A. Vourlidas, “Solar energetic particles in the inner heliosphere: status and open questions,” *Phil. Trans. R. Soc. A.*, vol. 377, no. 2148, p. 20180100, Jul. 2019, doi: 10.1098/rsta.2018.0100.

[17] L. Narici, A. Rizzo, F. Berrilli, and D. Del Moro, “Solar Particle Events and Human Deep Space Exploration: Measurements and Considerations,” in *Extreme Events in Geospace*, Elsevier, 2018, pp. 433–451. doi: 10.1016/B978-0-12-812700-1.00017-0.

[18] L. Walsh *et al.*, “Research plans in Europe for radiation health hazard assessment in exploratory space missions,” *Life Sciences in Space Research*, vol. 21, pp. 73–82, May 2019, doi: 10.1016/j.lssr.2019.04.002.

[19] National Aeronautics and Space Administration, “NASA space flight human-system standard volume 1, revision A: crew health,” NASA-STD-3001, Volume 1, 2014.

[20] U. Straube, T. Berger, and M. Dieckmann, “The ESA Active Dosimeter (EAD) system onboard the International Space Station (ISS),” *Zeitschrift für Medizinische Physik*, p. S0939388923000387, May 2023, doi: 10.1016/j.zemedi.2023.03.001.

[21] V. Benghin *et al.*, “Results of long-term radiation environment monitoring by the Russian RMS system on board Zvezda module of the ISS,” *Life Sciences in Space Research*, p. S2214552422001006, Nov. 2022, doi: 10.1016/j.lssr.2022.11.002.

[22] V. M. Petrov, D. A. Kartashov, Yu. A. Akatov, A. V. Kolomensky, and V. A. Shurshakov, “Comparison of space radiation doses inside the Matroshka-torso phantom installed outside the ISS with the doses in a cosmonaut body in Orlan-M spacesuit during EVA,” *Acta Astronautica*, vol. 68, no. 9–10, pp. 1448–1453, May 2011, doi: 10.1016/j.actaastro.2010.06.002.

[23] T. P. Dachev, “Analysis of the space radiation doses obtained simultaneously at two different locations outside the ISS,” *Advances in Space Research*, vol. 52, no. 11, pp. 1902–1910, Dec. 2013, doi: 10.1016/j.asr.2013.08.011.

[24] J. Semkova *et al.*, “Observation of radiation environment in the International Space Station in 2012–March 2013 by Liulin-5 particle telescope,” p. 11, 2014.

[25] M. R. Shavers *et al.*, “Implementation of ALARA radiation protection on the ISS through polyethylene shielding augmentation of the Service Module Crew Quarters,” *Advances in Space Research*, vol. 34, no. 6, pp. 1333–1337, Jan. 2004, doi: 10.1016/j.asr.2003.10.051.

[26] M. Kruglanski *et al.*, “Space Environment Information System (SPENVIS),” *Geophysical Research Abstracts*, vol. 11, p. 2, Apr. 2009.

[27] “SPENVIS - Space Environment, Effects, and Education System.” https://www.spenvis.oma.be/credits.php (accessed Aug. 26, 2022).

[28] D. K. Bond, B. Goddard, R. C. Singleterry, and S. Bilbao y León, “Evaluating the effectiveness of common aerospace materials at lowering the whole body effective dose equivalent in deep space,” *Acta Astronautica*, vol. 165, pp. 68–95, Dec. 2019, doi: 10.1016/j.actaastro.2019.07.022.

DOI: 10.13009/EUCASS2023-879

[29] "RayActive: An all-in-one R2S neutron induced activation analysis tool based on new intrinsic resolution methods.," *Nuclear Engineering and Design*, vol. 386, p. 111548, Jan. 2022, doi: 10.1016/j.nucengdes.2021.111548.

[30] Y. Akisheva *et al.*, "New Simulations for Radiation Shielding Materials in Lunar Habitats," presented at the 73rd International Astronautical Congress (IAC), Paris, France: International Astronautical Federation (IAF), Sep. 2022, pp. 1–7. Accessed: Jun. 14, 2023. [Online]. Available: https://iafastro.directory/iac/archive/browse/IAC-22/A5/1/72978/

[31] V. S. Engelschiøn *et al.*, "EAC-1A: A novel large-volume lunar regolith simulant," *Sci Rep*, vol. 10, no. 1, p. 5473, Dec. 2020, doi: 10.1038/s41598-020-62312-4.

[32] M. Durante and F. A. Cucinotta, "Physical basis of radiation protection in space travel," *Rev. Mod. Phys.*, vol. 83, no. 4, pp. 1245–1281, Nov. 2011, doi: 10.1103/RevModPhys.83.1245.

[33] ICRP, "1990 Recommendations of the International Commission on Radiological Protection," Annals of the ICRP Vol. 21, No. 1-3, 1991.